

# TECH SERIES

## The Solid Rocket Motor - Part 6 Erosive Burning Design Criteria for High Power and Experimental/Amateur Solid Rocket Motors

by Charles E. Rogers

### Introduction

This article is part of a continuing series in *High Power Rocketry Magazine* on the solid rocket motor. In this series solid propellant selection and characterization, internal ballistics and grain design, erosive burning design criteria, and solid rocket motor performance analysis and prediction will be covered in extensive detail. Previous installments of this series were published in the following issues of *High Power Rocketry Magazine*; *Performance Analysis of the Ideal Rocket Motor* (in retrospect Part "0" of the series), in the January 1997 issue; Parts 1 and 2, *Solid Propellant Selection and Characterization*, in the February (A) 2001 and February (B) 2001 issues; Part 3, *Solid Propellant Grain Design and Internal Ballistics*, in the October/November 2002 issue; and Parts 4 and 5, *Departures from Ideal Performance for Conical Nozzles and Bell Nozzles, Straight-Cut Throats and Rounded Throats*, in the October 2004 and November 2004 issues.

In this installment of the series erosive burning design criteria for high power and experimental/amateur solid rocket motors will be presented. Design criteria for motors that will essentially burn non-erosive, and design criteria for maximum recommended erosive burning will be presented. Combined core Mach number/core mass flux erosive burning design criteria will be presented which will allow the effective design of non-erosive and erosive solid rocket motors whether the motor propellant is sensitive to velocity-based or mass flux-based erosive burning. Of particular interest to high power and experimental/amateur rocketeers is that these erosive burning design criteria will allow the Length-to-Diameter ratio (L/D) of high power and experimental/amateur solid rocket motors to be

increased, or will allow an increase in the amount of propellant installed in a motor for a given motor L/D, increasing the motor installed performance in minimum diameter rockets and/or increasing the motor total impulse. Finally, a constant core mass flux core design will be presented that once a given level of erosivity or non-erosivity for the motor has been set, will allow a further increase in the motor L/D or motor installed propellant, and hence an even greater increase in motor performance.

The present author would like to give special thanks to Derek Deville from Environmental Aerosciences Corporation (EAC) for providing core mass flux erosive burning data from propellant characterization tests performed as part of the development of the solid rocket motor for the CSXT project, and Gary Rosenfield of AeroTech, Inc. and RCS Rocket Motor Components, Inc., for providing motor drawings from the RCS Resource Library Compact Disk (CD), modified versions of which were used in several of the figures in this article.

### Erosive Burning

When high velocity or high mass flow rate hot gas from upstream combustion passes over a downstream burning surface in a solid rocket motor a local increase in propellant burning rate results. This local increase in propellant burning rate is called erosive burning. The propellant burning rate ( $r_b$ ) in a particular location in a solid rocket motor consists of the non-erosive burning rate ( $r_0$ ), and an addition to the burning rate due to erosive burning ( $r_e$ ).

$$r_b = r_0 + r_e \quad (1)$$

Where:

$r_b$  = propellant burning rate, m/sec (in/sec)

$r_e$  = addition to propellant burning rate due to erosive burning, m/sec (in/sec)

$r_0$  = non-erosive propellant burning rate, m/sec (in/sec)

The non-erosive propellant burning rate is a function of chamber pressure. The most widely used analytical expression for the non-erosive propellant burning rate as a function of chamber pressure is de Saint Robert's law (Eq. (2)).

$$r_0 = a (\rho_c)^n \quad (2)$$

Where:

$a$  = coefficient of pressure, also called burning rate constant

$n$  = burning rate pressure exponent

$\rho_c$  = chamber pressure, Pa (lb/in<sup>2</sup>)

The coefficient of pressure (also called the burning rate constant) and the pressure exponent for the propellant are part of what is known as the propellant internal ballistic characteristics, which are empirically measured characteristics of the propellant, and which vary from propellant to propellant.

There are two basic types of erosive burning; velocity-based erosive burning and mass flux-based erosive burning. Some propellants are more sensitive to the effect of the velocity of the hot gas flowing over the burning surface of the propellant (velocity-based erosive burning), some propellants are more sensitive to the effect of the mass flux of the hot gas over the burning surface (mass flux-based erosive burning). Mass flux is the mass flow rate per square inch of port area (core cross-sectional area) flowing over the propellant burning surface. Mass flux is calculated by taking the propellant mass flow rate from the burning surfaces upstream of the location for which the mass flux is being determined, divided by the port area at the location for which the mass flux is being determined.

$$G = \dot{m}'_b / A_p \quad (3)$$

$$A_p = \pi r_c^2$$

Where:

$A_p$  = port area (core cross-sectional area), m<sup>2</sup> (in<sup>2</sup>)

$G$  = mass flux, kg/sec-m<sup>2</sup> (lb/sec-in<sup>2</sup>)

$\dot{m}'_b$  = propellant mass flow rate upstream of mass flux location, kg/sec (lb/sec)

$r_c$  = core radius (circular port), m (in)

As will be seen for velocity-based erosive burning the speed of the gas flow over the propellant burning surface will be characterized based on Mach number rather than velocity, as the Mach number can be directly tied to the motor core geometry and thus is a more intuitive and more direct parameter to track for velocity-based erosive burning. Whether the erosive burning of a propellant is velocity-dependent or mass flux-dependent can only be determined from erosive burning characterization tests.

The approach that will be presented in this article is the use of combined Mach number-based and mass flux-based erosive burning design criteria to assist in the design of solid rocket motors that have either essentially no erosive burning, or a reasonable amount of erosive burning for maximum performance with good design margins for safe operation of the motor. Since combined Mach number-based (replacing velocity) and mass flux-based erosive burning design criteria are used, these design criteria can be used for either velocity-sensitive or mass flux-sensitive erosive burning propellants, or for propellants where the sensitivity of the propellant to velocity-based and mass flux-based erosive burning has not yet been determined.

## Erosive Burning Motor Design Issues

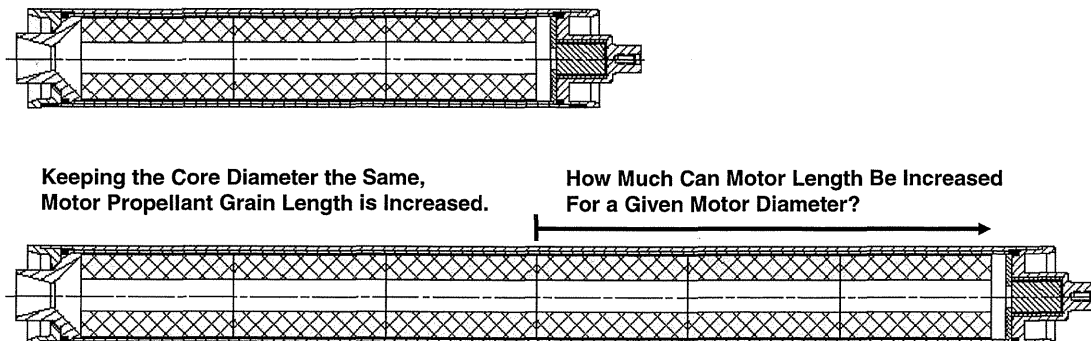
Figures 1 and 2 illustrate some of the solid rocket motor design issues that arise from erosive burning. From Figure 1 one of the primary high power and experimental/amateur rocket design techniques to maximize performance for minimum diameter rockets is to place the maximum motor total impulse behind the smallest possible rocket frontal area, producing the minimum aerodynamic drag for the rocket. The installed total impulse is maximized in the rocket for a given frontal area by lengthening the motor; i.e., by increasing the motor Length-to-Diameter ratio (L/D). Thus a primary question for the high power or experimental/amateur solid rocket motor designer is how high of an L/D can the motor be designed to; how much can the motor length be increased for a given motor diameter.

As will be seen later in this article, velocity-based erosive burning is a function of the port area (the core cross-sectional area) divided by the throat area (the port-to-throat area ratio). The lower the port-to-throat area ratio, the higher the velocity-based ero-

# Erosive Burning Motor Design Issues - 1

High Length-to-Diameter (L/D) Motors Increase Rocket Flight Performance.

Maximizes Total Impulse within a Given Frontal Area,  
Minimizes Aerodynamic Drag in Minimum Diameter Rockets.



For Velocity-Based Erosive Burning:

- 1) Increased Propellant Grain Length Increases Propellant Surface Area.
- 2) For Same  $K_n$ , Increased Propellant Surface Area Requires Increase in Throat Area ( $A_{th}$ ).
- 3) Increased Throat Area Approaches Port Area ( $A_p$ , the Core Cross-Sectional Area). Port-to-Throat Area Ratio ( $A_p/A_{th}$ ) Decreases, Core Mach Number Increases, Increased Velocity-Based Erosive Burning.

For Mass Flux-Based Erosive Burning:

- 1) Increased Propellant Grain Length Increases Propellant Surface Area.
- 2) Increased Propellant Surface Area Increases Mass Flow Rate Down Core.
- 3) With Same Core Diameter, Port Area (Core Cross-Sectional Area) Remains the Same. Increased Core Mass Flow Rate through Same Core Cross-Sectional Area Results in Increased Core Mass Flux, Increased Mass Flux-Based Erosive Burning.

Figure 1. Erosive Burning Motor Design Issues - 1.

sive burning. From Figure 1, when the motor length is increased for a given motor diameter (the motor L/D is increased), the motor grain length increases which increases the motor propellant burning surface area. If the motor  $K_n$  (the propellant burning surface area divided by the throat area,  $A_b/A_{th}$ ) is kept constant to maintain the same motor chamber pressure, as the propellant burning surface area is increased the motor throat area will have to increase to maintain the same motor  $K_n$ . If the motor core diameter is held constant, as the motor throat area is increased with the same port area, the port-to-throat area ratio will be decreased. This reduced port-to-throat area ratio will increase velocity-based erosive burning, which will set a limit to how much the motor length (and motor L/D) can be increased.

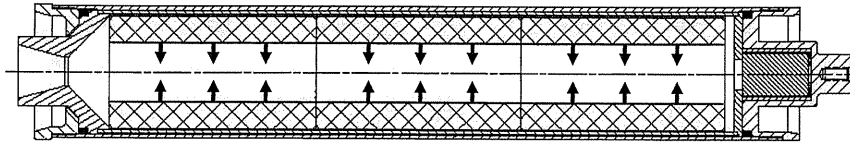
As will be seen later in this article, mass flux-based erosive burning is a function of the core mass flux  $G$  (Eq. (3)), the mass flow rate in the core divided by the port area (the core cross-sectional area). The higher the core mass flux, the higher the mass flux-based erosive burning. From Figure 1, when the motor length is increased for a given motor diame-

ter, the increased motor grain length will increase the propellant burning surface area, increasing the mass flow rate in the core. If the motor core diameter is held constant, when this increased mass flow rate passes through the same port area (the same core cross-sectional area), the mass flux in the core will increase, increasing mass flux-based erosive burning. This increased mass flux-based erosive burning will set a limit to how much the motor length can be increased.

From Figure 2 another solid rocket motor design technique to increase the performance of high power and experimental/amateur rockets is to reduce the core diameter for a given motor length and diameter. Given a fixed motor case length and diameter (a fixed motor outside envelope and internal volume), if the core diameter is decreased there will be additional installed propellant in the motor, thus an increased total impulse for the motor. Note that even for a high L/D motor like that shown in Figure 1, once the motor length has been set, decreasing the motor core diameter increases the amount of propellant installed in the motor, increasing the motor total impulse. Thus for any motor (short or long, low

## Erosive Burning Motor Design Issues - 2

For Any Motor Length (Short or Long), Reducing Core Diameter Increases Propellant Loading, More Propellant Loaded within Fixed Motor Volume. Maximizes Volumetric Loading (Total Impulse Installed within a Fixed Volume). Increased Rocket Flight Performance from Higher Total Impulse Installed within Volume or Length Available for Motor.



How Much Can Motor Core Diameter Be Reduced?

For Velocity-Based Erosive Burning:

- 1) Reduced Core Diameter Reduces Port Area ( $A_p$ , the Core Cross-Sectional Area). Port Area Begins to Approach Fixed Throat Area ( $A_{th}$ ). Port-to-Throat Area Ratio ( $A_p/A_{th}$ ) Decreases, Core Mach Number Increases.
- 2) Increased Core Mach Number, Increased Velocity-Based Erosive Burning.

For Mass Flux-Based Erosive Burning:

- 1) Reduced Core Diameter Reduces Propellant Surface Area, Reducing Core Mass Flow Rate, but Port Area (Core Cross-Sectional Area) is Reduced at a Greater Rate. Result is an Increase in Core Mass Flux.
- 2) Increased Core Mass Flux, Increased Mass Flux-Based Erosive Burning.

Figure 2. Erosive Burning Motor Design Issues - 2.

L/D or high L/D), once the motor length and diameter and thus the motor volume have been fixed, decreasing the core diameter increases the motor total impulse.

As noted previously, for velocity-based erosive burning the lower the port-to-throat area ratio, the higher the velocity-based erosive burning. If the motor throat area is held constant, for essentially the same  $K_n$  and thus essentially the same chamber pressure, as the core diameter is decreased the port-to-throat area ratio will decrease, increasing velocity-based erosive burning. This increased velocity-based erosive burning will set a limit to how much the core diameter can be decreased.

From Figure 2, for mass flux-based erosive burning as the core diameter is reduced, there is a decrease in the mass flow rate in the core because the propellant burning surface area in the core (ignoring the propellant burning surfaces on the sides of the individual grains in Figure 2) is decreased. The propellant burning surface area in the core is directly proportional to the core radius  $r_c$  (the core propellant burning surface area is equal to the circumference of the core [ $2\pi r_c$ ] times the length of the core), as the core diameter decreases the core propellant burning surface area decreases. But the port area (the core cross-sectional area,  $\pi r_c^2$ ) decreases at a faster rate, as the port area is directly proportional to the core radius squared. The net effect of a decrease in core diameter is an increase in core mass flux, increasing mass flux-based erosive burning. This increased mass flux-based erosive burning will set a limit to how much the motor

core diameter can be decreased.

How much the motor L/D can be increased for a given motor diameter, and how much the core diameter can be decreased for a given motor length and volume, are important design issues facing high power and experimental/amateur solid rocket motor designers. After the basic motor design and the overall grain geometry design are completed, the motor designer faces a fundamental issue, how small or large does the motor core need to be? In this article design criteria will be presented for velocity-based and mass flux-based erosive burning, including combined core Mach number/core mass flux design criteria which will allow solid rocket motor designers to configure motor cores for either essentially non-erosive burning, or to achieve maximum recommended, yet conservative erosivity in the motor core design.

### Velocity-Based Erosive Burning

Data showing the typical augmentation of propellant burning rate with combustion gas velocity for composite propellants sensitive to velocity-based erosive burning is presented in Figure 3 (reproduced from Ref. 1, original reference Ref. 2). The combustion gas velocity ( $u_g$ ) is the local velocity of the hot gas flow down the core of the solid rocket motor, which varies from zero velocity at the head end of the core to a maximum velocity at the aft end of the core. The vertical scale is the ratio of the propellant burning rate including erosive burning ( $r_b$ , see Eq.

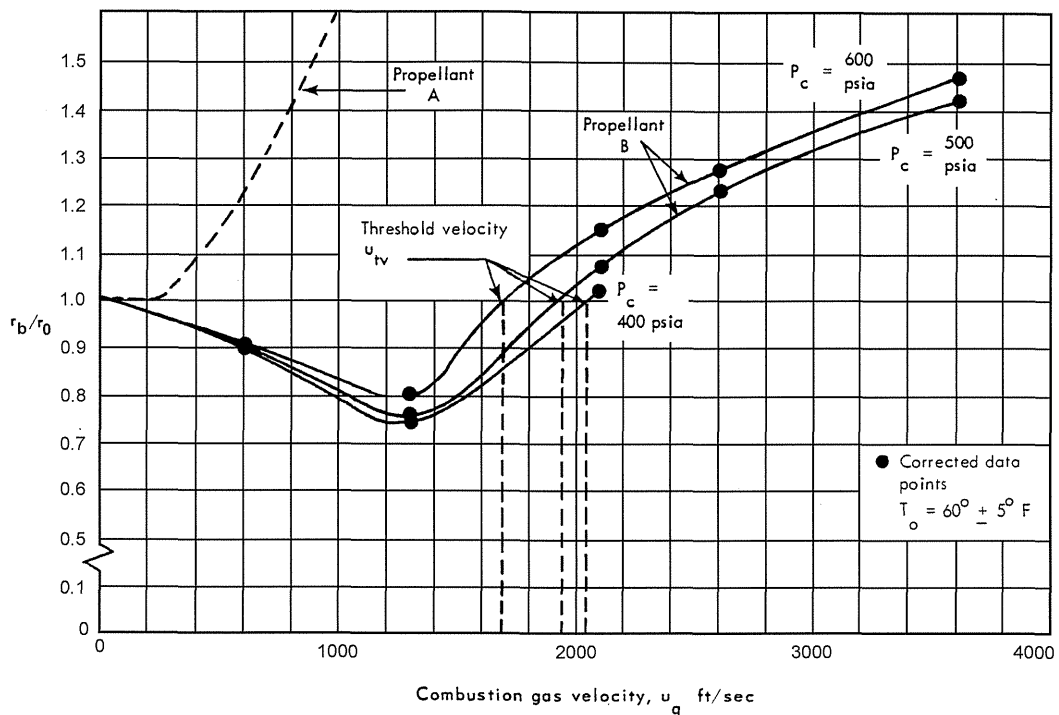


**Figure 3. Typical Effect of Combustion Gas Velocity on Burning Rate Augmentation — Velocity-Based Erosive Burning.**

(1) divided by the non-erosive burning rate ( $r_0$ ).  $r_b/r_0 = 1.0$  indicates non-erosive burning.

Note from Figure 3 that at low velocity the propellant burning rate actually dips below the assumed non-erosive value. This opens up the interesting possibility that experimental/amateur rocketeers may be performing propellant characterization tests with the core gas flow velocities too low, and while assuming that they are measuring the non-erosive propellant burning rate, are actually measuring a lower propellant burning rate from the dip in the curve in Figure 3. The present author, for the various propellant characterization tests he has participated in, has never seen this phenomenon of the dip in propellant burning rate shown in Figure 3. Experimental/amateur rocketeers when performing propellant characterization tests should add additional tests to verify that this possible dip in propellant burning rate shown in Figure 3 is not occurring for the propellant being tested. Techniques for checking for a possible dip in propellant burning rate at low core gas flow velocities when performing propellant characterization tests will be presented later in this article.

The threshold velocity ( $u_{tv}$ ) is the combustion gas velocity where velocity-based erosive burning begins. From Figure 3 the threshold velocity for Propellant B varies from 1700 ft/sec to 2050 ft/sec as a function of chamber pressure. As shown in Figure 3 for Propellant B, the higher the motor chamber pressure the lower the propellant threshold velocity. Figure 3 also shows the possible wide vari-

ation in threshold velocity between two different propellants (Propellants A and B), again emphasizing that velocity-based erosive burning is propellant dependent, and can vary widely from propellant to propellant.

Using analysis methods that will be subsequently presented, the experimental/amateur rocketeer can calculate the local flow velocity at the aft (nozzle) end of the core of the solid rocket motor, and can compare the flow velocity to the threshold velocity as a function of chamber pressure in Figure 3. As will be seen the Mach number at the aft end of the core, which is the region which has the highest level of erosive burning, is a function of the ratio of the port area to the throat area. Using the Mach number at the aft end of the core as an erosive burning limit and design criteria is much more useful than using flow velocity, and the present author recommends that the Mach number at the aft end of the core be used as the primary design criteria for velocity-based erosive burning.

### **Core Mach Number Design Criteria for Velocity-Based Erosive Burning**

The threshold velocity where velocity-based erosive burning begins of 1700 ft/sec to 2050 ft/sec shown in Figure 3 at first appears quite high. With choked flow at the nozzle throat (Mach 1 at the nozzle throat), the flow in the solid rocket motor core

will be subsonic. It should be remembered that the temperature of the gas flow in the motor core, due to the combustion of the solid propellant, is quite high, 2000-6500 °R (1540-6040 °F). Thus the speed of sound for the gas flow in the motor core will be quite high.

The speed of sound is a function of the ratio of specific heats, a gas constant, and temperature. The gas constant ( $R$ ) is the universal gas constant ( $R'$ ) divided by the molecular mass  $\bar{M}$ .

In SI Units:

$$a = \sqrt{\gamma R T} \quad (4)$$

$$R = R' / \bar{M}$$

Where:

$a$  = speed of sound, m/sec

$\bar{M}$  = molecular mass, kg/kg-mol

$R$  = gas constant per unit weight, J/kg-°K

$R'$  = universal gas constant, 8314.3 J/kg mol-°K

$T$  = absolute temperature, °K

$\gamma$  = ratio of specific heats, dimensionless

If English Units are used the molecular mass is replaced with molecular weight. To calculate the speed of sound for the gas flow in the motor core, the ratio of specific heats and the gas constant (the universal gas constant divided by the molecular mass) for the combustion products making up the gas flow in the core are used in Eq. (4). The temperature used in Eq. (4) is the adiabatic equilibrium flame temperature ( $T_c$ ), the combustion temperature. When several values are available from thermochemical equilibrium theoretical specific impulse programs for adiabatic equilibrium flame temperature, ratio of specific heats, and the gas properties (typically for the chamber, throat, and nozzle exit), the chamber values should be used in Eq. (4) for the speed of sound calculations for the gas flow in the motor core.

Table 1 presents speed of sound data for representative composite solid propellants, and representative high power and experimental/amateur solid propellants for the gas flow in the core of a solid rocket motor. The propellant adiabatic equilibrium flame temperature and gas properties used in Eq. (4) for the speed of sound are included in Table 1. Two of the propellants are representative composite solid propellants taken from Sutton, *Rocket Propulsion*

*Elements* (Ref. 3), the rest of the propellant data is from Appendix A of Parts 1 and 2 of *The Solid Rocket Motor* series (Ref. 4).

Note from the data in Table 1 that the speed of sound for the gas flow in the motor core is primarily a function of the propellant adiabatic equilibrium flame temperature, and that the speed of sound for the gas flow in the motor core is quite high, 2000-3500 ft/sec.

Based on the Propellant B data in Figure 3, using a representative chamber pressure of 500 psia, a representative threshold velocity ( $u_{tv}$ ) for the onset of velocity-based erosive burning is 1950 ft/sec. Using a 20% increase in propellant burning rate ( $r_b/r_0 = 1.2$ ) as a reasonable upper bound for maximum recommended erosivity for velocity-based erosive burning, based on the data plotted in Figure 3 for Propellant B at a chamber pressure of 500 psia, the combustion gas velocity ( $u_g$ ) for maximum recommended erosivity for velocity-based erosive burning is 2500 ft/sec. These two velocity limits can be converted to Mach number limits by dividing velocity by the speed of sound.

$$(M_a)_{tv} = u_{tv} / a \quad (5)$$

$$(M_a)_g = u_g / a \quad (6)$$

Where:

$(M_a)_g$  = Mach number for flow in motor core based on combustion gas velocity, dimensionless

$(M_a)_{tv}$  = threshold Mach number for flow in motor core based on threshold velocity for onset of velocity-based erosive burning, dimensionless

$u_g$  = combustion gas velocity, m/sec (ft/sec)

$u_{tv}$  = threshold velocity for onset of velocity-based erosive burning, m/sec (ft/sec)

Note that the threshold velocity for velocity-based erosive burning and the velocity for the maximum recommended erosivity can occur anywhere in the motor core, but they will be reached first in the highest velocity location in the core which is at the aft (nozzle) end of the core. Thus the Mach number of interest is the Mach number at the aft end of the core, where the Mach number and the combustion gas velocity will be highest and where there will be the highest level of velocity-based erosive burning,

Propellant	AeroTech/ISP Propellant I.D. Number (Notes 1, 2)	$T_c$ (°R) (Note 3) (Note 4)	$T_c$ (°K) (Note 3) (Note 4)	$\gamma$ (Note 4)	$\bar{M}$ (kg/mol) (Note 4)	$a$ (ft/sec) (Note 4)	$(M_a)_{tv}$ ( $u_{tv} =$ 1950 ft/sec) (Note 5)	$(M_a)_g$ ( $u_g =$ 2500 ft/sec) (Note 6)
AeroTech/ISP High Solids Loading High Specific Impulse	8843	6377	3542.8	1.13	29.43	3489.3	0.56	0.72
Organic Polymer Binder/AP/AL 18% Binder 66-78% AP 4-20% AL (Sutton [Ref. 3])	NA	5068.8	2816	1.21	25.0	3492.7	0.56	0.72
Polymer Binder/ AP/AL 12% Binder 68-84% AP 4-20% AL (Sutton [Ref. 3])	NA	6067.8	3371	1.17	29.3	3471.0	0.56	0.72
AeroTech Blue Thunder	8121	4464	2480	1.23	23.06	3440.9	0.57	0.73
AeroTech White Lightning	8225	4108	2282.2	1.15	27.56	2919.5	0.67	0.86
AeroTech Black Jack	8021D/ 8023D	2390	1327.8	1.17	31.67	2095.3	0.93	Over 1.0

Notes:

- (1) All AeroTech/ISP propellants use Hydroxy-Terminated Polybutadiene (HTPB) binder and Ammonium Perchlorate (AP) oxidizer.
- (2) First two numbers of Propellant I.D. Number are solids loading. Example; 8843 - 88% solids loading (12% HTPB binder).
- (3) Adiabatic equilibrium flame temperature.
- (4)  $p_c = 1000$  psia, equilibrium flow.
- (5) Core Mach number for threshold velocity ( $u_{tv} = 1950$  ft/sec) for onset of velocity-based erosive burning.
- (6) Core Mach number for combustion gas velocity for maximum recommended erosivity ( $u_g = 2500$  ft/sec) for velocity-based erosive burning

NA = Not Applicable

AL = aluminum

AP = ammonium perchlorate

HTPB = hydroxyl-terminated polybutadiene

**Table 1. Adiabatic Equilibrium Flame Temperature, Ratio of Specific Heats, Gas Properties, Speed of Sound, and Velocity-Based Erosive Burning Threshold and Maximum Recommended Erosivity Mach Number Limits for Representative Composite Solid Propellants and High Power and Experimental/Amateur Solid Propellants.**

Propellant	$\rho_c$ (psia)	$T_c$ (°R)	$T_c$ (°K)	$\gamma$	$\bar{M}$ (kg/mol)	$a$ (ft/sec)	
Metalized HTPB/AP 82% Solids Loading	1000	4210.2	2339.0	1.243	27.13	3097.0	
	500	4144.3	2302.4	1.245	26.96	3084.9	0.4% decrease in speed of sound for combustion gas flow in core.

**Table 2. Variation of Adiabatic Equilibrium Flame Temperature, Ratio of Specific Heats, Gas Properties, and Speed of Sound with Chamber Pressure for Combustion Gas Flow for a Representative Composite Solid Propellant.**

and which fortuitously as it turns out is the Mach number in the core that is the easiest to calculate.

Because the core Mach number at the aft end of the core is used almost exclusively over the Mach numbers elsewhere in the core, the term "core Mach number at the aft end of the core" is often truncated to just "core Mach number," in particular when describing a motor design. It is important to remember that when a motor design is stated to have a design "core Mach number," this "core Mach number" is the Mach number at the aft end of the core at motor ignition.

Core Mach number limits based on the threshold velocity for velocity-based erosive burning and the velocity for maximum recommended erosivity are included for the example propellants in Table 1.

Note that for the AeroTech/ISP propellants in Table 1 the adiabatic equilibrium flame temperature, ratio of specific heats and gas properties were calculated based on  $\rho_c = 1000$  psia, while the representative threshold velocity for the onset of velocity-based erosive burning and the maximum recommended erosivity gas flow velocity were based on  $\rho_c = 500$  psia. (Both chamber pressures based on the available data.) The chamber pressure for the representative composite solid propellant data from Sutton, *Rocket Propulsion Elements*, was not specified. The  $\rho_c = 1000$  psia adiabatic equilibrium flame temperature data, ratio of specific heats and gas properties data can still be used for the speed of sound calculations and the  $(M_a)_{iv}$  and  $(M_a)_g$  calculations in Table 1 because there is little variation in the adiabatic equilibrium flame temperature, the ratio of specific heats and the gas properties with chamber pressure. Table 2 shows the variation in the adiabatic equilibrium flame temperature, the ratio of specific heats, the gas properties, and the speed of sound for the combustion gas flow as a function chamber pressure for a representative metalized HTPB/AP composite propellant. Note that

decreasing the chamber pressure from 1000 psia to 500 psia reduces the speed of sound only 0.4%.

Based on the data presented in Table 1, the present author recommends the following core Mach number design criteria for velocity-based erosive burning for high power and experimental/amateur solid rocket motors:

Non-Erosive:

$$\text{Core Mach Number} \leq 0.50$$

Maximum Recommended Erosivity:

$$\text{Core Mach Number} = 0.70$$

From Table 1 it can be seen that many of the propellants have a speed of sound for the combustion gas flow in the motor core of 3400-3500 ft/sec, which when combined with the threshold velocity for the onset of velocity-based erosive burning of 1950 ft/sec, results in a core Mach number of 0.56-0.57. For design margin on avoiding the onset of velocity-based erosive burning the present author sets a non-erosive core Mach number limit that is reduced approximately 10% to a core Mach number of 0.50. From Table 1 the 2500 ft/sec combustion gas velocity for maximum recommended erosivity for velocity-based erosive burning, combined with the speed of sound of 3400-3500 ft/sec for many of the propellants in Table 1, results in a core Mach number of 0.72-0.73, rounded down by the present author to 0.70. Note from Table 1 that the highest adiabatic equilibrium flame temperature propellants set the lowest core Mach number limits. For the lower adiabatic equilibrium flame temperature propellants Table 1 shows that the core Mach number limits are higher, thus using core Mach number limits based on the highest propellant adiabatic equilibrium flame temperatures sets conservative core

Mach number limits for all propellants.

Could the maximum recommended erosivity core Mach number be increased, for a more aggressive design in terms of velocity-based erosive burning? As will be shown in the next section, with a core Mach number of 0.70 the port area (the core cross-sectional area) is only 10% larger than the throat area. If the port area is reduced to the throat area, the motor will fire nozzleless; i.e. at ignition Mach 1 will be reached at the end of the core rather than at the throat. Thus with a core Mach number of 0.70 the port area is nearly as small as the throat area, and thus little can be gained from further reductions in the port area, and what gains could be made (10% or less) would come at the cost of much more risk in terms of much higher velocity-based erosive burning at ignition of the motor.

### Core Mach Number as a Function of Port-to-Throat Area Ratio

The Mach number at the aft (nozzle) end of the core can be determined from the port area (the core cross-sectional area) divided by the throat area (the port-to-throat area ratio) using Eq. (7) from Section 6.5.2 of *Space Propulsion Analysis and Design* (Ref. 5).

$$\frac{A_p}{A_{th}} = \frac{1}{M_a} \left[ \frac{2 + (\gamma - 1)M_a^2}{1 + \gamma} \right]^{(\gamma + 1)/2(\gamma - 1)} \quad (7)$$

$$A_p = \pi r_c^2$$

$$A_{th} = \pi r_{th}^2$$

Where:

$$A_p = \text{port area (core cross-sectional area),} \\ \text{m}^2 \text{ (in}^2\text{)}$$

$$A_{th} = \text{nozzle throat area (throat cross-sectional} \\ \text{area), m}^2 \text{ (in}^2\text{)}$$

$$A_p/A_{th} = \text{port-to-throat area ratio, dimensionless}$$

$$M_a = \text{core Mach number at aft end of core,} \\ \text{dimensionless}$$

$$r_c = \text{core radius (circular port), m (in)}$$

$$r_{th} = \text{nozzle throat radius, m (in)}$$

Eq. (7) gives the core Mach number at the aft end of the core, which as discussed previously is known

as the "core Mach number." The ratio  $A_p/A_{th}$  is the port-to-throat area ratio, and is a key parameter for the motor, as it determines the core Mach number.

Using Eq. (7) if the desired core Mach number is known, and the port-to-throat area ratio ( $A_p/A_{th}$ ) needs to be determined, the core Mach number can simply be entered into Eq. (7) to determine the port-to-throat area ratio. The more common situation is that the port-to-throat area ratio is known, and it is the core Mach number that needs to be determined. Simple iterative methods can be used to solve Eq. (7) for the core Mach number given the port-to-throat area ratio, with the simplest method being simply iterating the core Mach number from zero using an increment of 0.01 until the port-to-throat area ratio is matched.

Note that since Eq. (7) is for the Mach number at the aft end of the core for the combustion gas flow down the core, that if several ratios of specific heats are available, the chamber value should be used, versus using the throat or nozzle exit values.

Note that the derivation of Eq. (7) from Ref. 5 assumes a constant port area, i.e., a constant cross-sectional area of the core. A more complex method for tapered cores is presented in Section 6.5.2 of Ref. 5. All cores that have erosive burning at ignition will have a tapered core later in the burn, and later in this article core designs will be presented that feature an increase in port area for the grains at the aft end of the motor, but the present author recommends that Eq. (7) be used for all solid rocket motors for determining the core Mach number, with the caveat that the equation is exact for constant cross-sectional area cores and non-erosive motors, and approximate for tapered or staggered cores and highly erosive motors.

Eq. (7) is somewhat complex, and needs to be solved iteratively, although the equation can be built into motor simulation programs. For core Mach number-based erosive burning design criteria the core Mach number is only needed at the aft end of the core and only at ignition, thus hand calculations can be performed using Eq. (7) using the motor grain geometry at ignition. Eq. (7) can be solved iteratively using hand calculations, but to simplify the process the present author has created Figure 4. Figure 4 is a plot of the core Mach number as a function of  $A_p/A_{th}$  based on Eq. (7) assuming a ratio of specific heats ( $\gamma$ ) equal to 1.2 (a good representative value for solid rocket motors). Experimental/ama-teur rocketeers can use Figure 4 for rapid determination of core Mach number for a given  $A_p/A_{th}$  at motor ignition.

Using Eq. (7), and assuming  $\gamma = 1.2$ , the previously recommended core Mach number design criteria can be converted to the following recommended port-to-throat area ratios ( $A_p/A_{th}$ ) for velocity-based

$M_a$  versus  $\frac{A_p}{A_{th}}$ ;  $\gamma = 1.2$

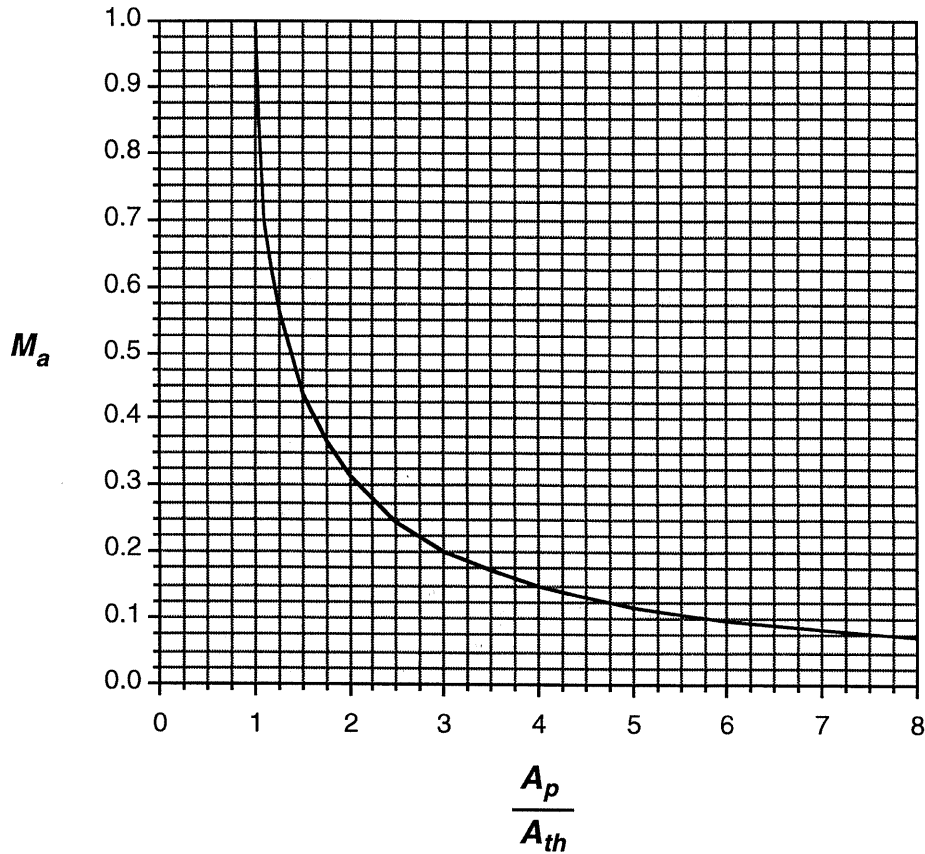


Figure 4.  $M_a$  as a function of  $A_p/A_{th}$ ,  $\gamma = 1.2$ .

erosive burning for high power and experimental/amateur solid rocket motors:

Non-Erosive:

Core Mach Number  $\leq 0.50$

For  $\gamma = 1.2$ ;  $A_p/A_{th} \geq 1.36$

Maximum Recommended Erosivity:

Core Mach Number = 0.70

For  $\gamma = 1.2$ ;  $A_p/A_{th} = 1.10$

Note that for the maximum recommended erosivity core Mach number of 0.70 the port area is only 10% larger than the throat area. Little therefore can be gained from further reductions in the port area. If the port area is reduced to the throat area the motor will fire nozzleless (Mach 1 at the end of the

core). The slope of the core Mach number with port-to-throat area ratio ( $A_p/A_{th}$ ) shown in Figure 4 becomes very steep for port-to-throat area ratios approaching 1.0, reaching very high core Mach numbers for port-to-throat area ratios less than 1.10. Thus as the port area approaches the throat area and the port-to-throat area ratio approaches 1.0, the velocity-based erosive burning will become very severe, not making it worth taking advantage of a further possible 10% reduction in port area.

### Mass Flux-Based Erosive Burning

Figure 5 (reproduced from Ref. 1, original reference Ref. 6) shows the typical augmentation of propellant burning rate with mass flux for a composite propellant sensitive to mass flux-based erosive burning. The mass flux shown on the horizontal scale is the mass flux over a particular section of the propellant. For downstream (towards the nozzle

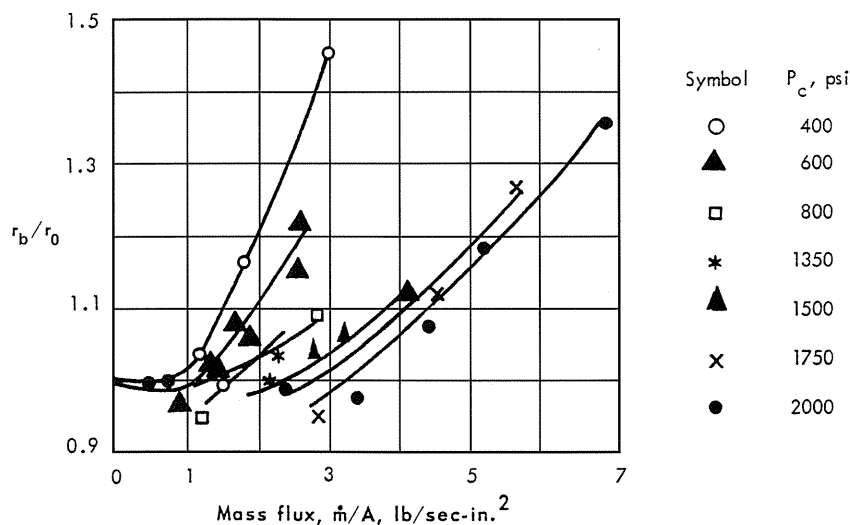


**Figure 5. Typical Effect of Mass Flux on Burning Rate Augmentation — Mass Flux-Based Erosive Burning.**

end) sections of the propellant grain the mass flux over the section arises from the mass flow from non-erosive burning, and the additional mass flow from any erosive burning that may be occurring further upstream in the core. As in Figure 3 the vertical scale is the ratio of the propellant burning rate including erosive burning ( $r_b$ ) divided by the non-erosive burning rate ( $r_0$ ).  $r_b/r_0 = 1.0$  indicates non-erosive burning.

One of the items of interest in Figure 5 is the mass flux for the onset of mass flux-based erosive burning (the threshold mass flux,  $G_{IV}$ ). As can be seen in Figure 5, the mass flux for the onset of mass flux-based erosive burning is a function of chamber pressure; the higher the chamber pressure the higher the mass flux required for the onset of erosive burning. Table 3 presents summary data for the threshold mass flux for the onset of mass flux-based erosive burning based on the data for the representative composite propellant plotted in Figure 5.

Note from Table 3 that the threshold mass flux for the onset of mass flux-based erosive burning is the same for both  $p_c = 1350$  psia and  $p_c = 1500$  psia, for which the present author has no explanation beyond possible scatter in the experimental data. The present author recommends that the threshold mass flux value of 2.15 lb/sec-in<sup>2</sup> be used for  $p_c = 1400$  psia, an approximate average of 1350 psia and 1500 psia.

The increase with chamber pressure of the threshold mass flux ( $G_{IV}$ ) for the onset of mass flux-based erosive burning is quite apparent from the data plotted in Figure 5 and the summary data in Table 3. Higher chamber pressures can allow the motor designer to design to a higher core mass flux and

still avoid mass flux-based erosive burning. Also apparent from the data plotted in Figure 5 is that a core mass flux  $\leq 1.0$  lb/sec-in<sup>2</sup> is non-erosive for all chamber pressures for the particular propellant plotted in Figure 5. The present author proposes that a core mass flux  $\leq 1.0$  lb/sec-in<sup>2</sup> will likely be non-ero-

$p_c$ Chamber Pressure (psia)	$G_{IV}$ Mass Flux for Onset of Mass Flux-Based Erosive Burning (lb/sec-in <sup>2</sup> )
400	1.0
600	1.15
800	1.8
1350	2.15 (Note 1)
1500	2.15 (Note 1)
1750	3.35
2000	3.65

Notes:

(1) Present author recommends that these two data points be replaced with a mass flux of 2.15 lb/sec-in<sup>2</sup> at  $p_c = 1400$  psia.

**Table 3. Threshold Mass Flux for the Onset of Mass Flux-Based Erosive Burning as a Function of Chamber Pressure.**

sive for all solid propellants at all chamber pressures.

Based on the data presented in Figure 5 and Table 3, the present author recommends the following core mass flux design criteria for mass flux-based erosive burning for high power and experimental/amateur solid rocket motors:

Non-Erosive:

$$\rho_c = 400\text{-}600 \text{ psia}; \\ \text{Core Mass Flux} \leq 1.0 \text{ lb/sec-in}^2$$

$$\rho_c = 800 \text{ psia}; \text{Core Mass Flux} \leq 1.75 \text{ lb/sec-in}^2$$

$$\rho_c = 1400 \text{ psia}; \text{Core Mass Flux} \leq 2.0 \text{ lb/sec-in}^2$$

Maximum Recommended Erosivity:

$$\rho_c = 400 \text{ psia}; \text{Core Mass Flux} = 2.0 \text{ lb/sec-in}^2$$

$$\rho_c = 600 \text{ psia}; \text{Core Mass Flux} = 2.5 \text{ lb/sec-in}^2$$

$$\rho_c \geq 800 \text{ psia}; \text{Core Mass Flux} = 3.0 \text{ lb/sec-in}^2$$

Core Mass Flux limits for Maximum Recommended Erosivity should not be exceeded unless Erosive Burning Characterization Tests are performed for propellant.

To arrive at the above core mass flux design criteria generally the core mass flux values from Figure 5 and Table 3 have been rounded to the nearest 0.25 lb/sec-in<sup>2</sup>. The present author has also been somewhat conservative in setting the above design criteria due to the steep slopes and uncertainty/scatter in the data at some chamber pressures for the data presented in Figure 5. Generally the maximum recommended erosivity core mass flux values are set based on a 20% increase in propellant burning rate ( $r_b/r_0 = 1.2$ ), again set conservatively due to the steep slopes of the propellant erosive burning rate with mass flux at some chamber pressures. (The  $\rho_c = 400$  psia data being an excellent example; if the curve is shifted to the left by 0.5 lb/sec-in<sup>2</sup> due to variations between propellants, there can be a major misprediction in the erosive burning rate.) Note that while the  $\rho_c = 1750$  psia data is clearly non-erosive at a core mass flux of approximately 3.0 lb/sec-in<sup>2</sup> and would have a  $r_b/r_0 = 1.2$  at 5.0 lb/sec-in<sup>2</sup>, the data above  $\rho_c = 800$  psia ( $\rho_c = 1350\text{-}1500$  psia) is inconclusive, and in terms of maximum recommended erosivity the present author recommends that a core mass flux of 3.0 lb/sec-in<sup>2</sup> not be exceeded even at high chamber pressures unless empirical mass flux-based erosive burning data is available for the propellant.

For the core mass flux design criteria that has been presented, the present author recommends that the maximum recommended erosivity core mass flux limits not be exceeded unless erosive burning characterization tests are performed to obtain empirical data for mass flux-based erosive burning for the particular propellant, to determine the actual threshold mass flux for the onset of mass flux-based erosive burning, and to determine a reasonable maximum mass flux limit for mass flux-based erosive burning.

### **CSXT D8 Propellant Mass Flux-Based Erosive Burning Characterization Data**

As part of the motor development program undertaken by the Environmental Aerosciences Corporation (EAC) for the Civilian Space eXploration Team (CSXT) experimental/amateur rocket, the first non-professional/non-governmental rocket launched into space which reached an altitude of 379,900 feet (72 miles), a series of propellant characterization tests were performed by Derek Deville of EAC, with consultation by the present author, to characterize the propellant for the CSXT solid rocket motor. Propellant characterization tests for chamber pressure versus  $K_n$  and burn rate versus chamber pressure were performed. Additionally mass flux-based erosive burning characterization tests were also performed, the results from which are presented in Figure 6. Figure 6 presents the burn rate versus chamber pressure for the CSXT D8 propellant, including the basic non-erosive propellant burn rate, and the variation of propellant burn rate with core mass flux. Note that the mass flux values listed in Figure 6 are core mass flux. Additionally note that using a technique recommended in a later section of this article, the mass flux values listed in Figure 6 and referred to below are the initial core mass flux at motor ignition at the aft (nozzle) end of the core, calculated based on the mass flow rate down the core being equal to the propellant flow rate, with the propellant flow rate calculated based on the propellant non-erosive burning rate at the test chamber pressure (core mass flux at ignition based on non-erosive burn rate).

Due to the tight development schedule for the CSXT solid rocket motor, there was time to perform only a limited number of propellant erosive burning characterization tests. Thus for the burn rate versus chamber pressure and core mass flux data for the CSXT D8 propellant presented in Figure 6, both the core mass flux and the chamber pressure were varied during the tests, versus the more rigorous technique of performing multiple mass flux tests at the same chamber pressure. The basic non-erosive burn

**CSXT D8 PROPELLANT BURN RATE VERSUS CHAMBER PRESSURE  
WITH VARIATION WITH CORE MASS FLUX  
(MASS FLUX-BASED EROSIVE BURNING)**

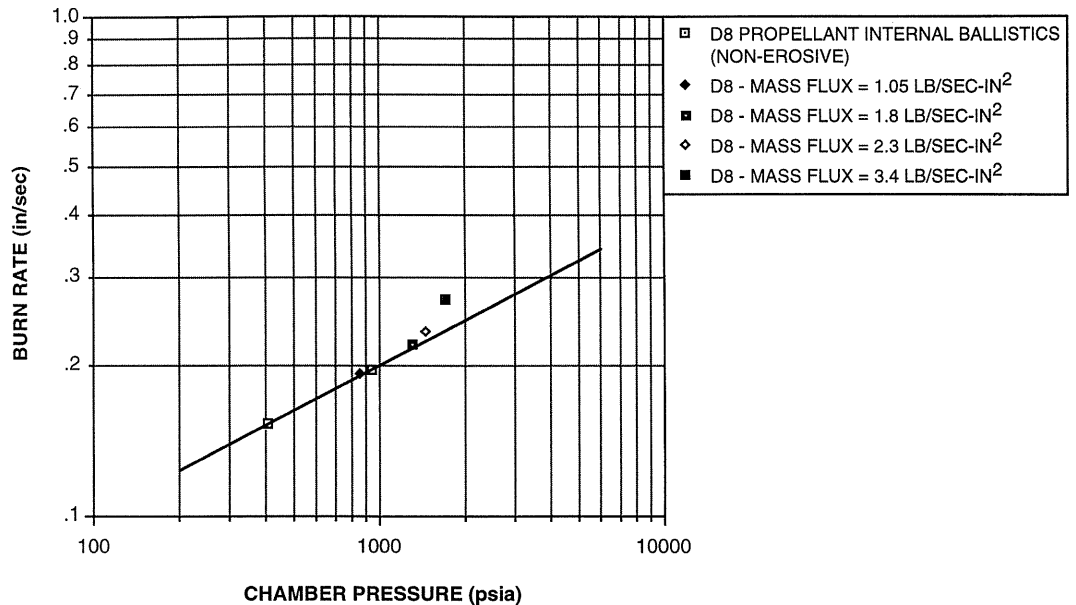


**Figure 6. CSXT D8 Propellant Burn Rate Versus Chamber Pressure with Variation with Core Mass Flux.**

rate versus chamber pressure for the D8 propellant is shown as a straight line on the log-log plot in Figure 6. The  $p_c = 409$  psia data point had an initial core mass flux of  $0.86 \text{ lb/sec-in}^2$  (less than  $1.0 \text{ lb/sec-in}^2$ , clearly non-erosive), the  $p_c = 933.4$  psia data point had an initial core mass flux of  $1.69 \text{ lb/sec-in}^2$ . For the  $p_c = 933.4$  psia data point the core mass flux initially looks high for a non-erosive burn rate test, but using the previously presented non-erosive core mass flux design criteria with a  $p_c = 933.4$  psia the threshold core mass flux for the beginning of mass flux-based erosive burning would be expected to be between  $1.75 \text{ lb/sec-in}^2$  and  $2.0 \text{ lb/sec-in}^2$ , making the  $p_c = 933.4$  psia data point also non-erosive.

Note that the data plotted in Figure 6 is the average burn rate and the average chamber pressure from each of the propellant characterization test motors fired. As the propellant characterization test motors were designed to produce a nearly flat thrust-time curve (a nearly constant thrust and chamber pressure), for the non-erosive tests there is little error from using the average burn rate and average chamber pressure versus any instantaneous values for the burn rate and chamber pressure with time during each test. Once the threshold mass flux for mass flux-based erosive burning is exceeded, the actual erosive burn rate at ignition of the propellant characterization test motor will be higher than the average burn rate value shown in Figure 6. The pro-

pellant characterization test motors were designed with a short burn time to minimize this effect, but it is important to note that while the threshold mass flux for mass flux-based erosive burning from Figure 6 is accurate, once mass flux-based erosive burning begins the actual erosive burn rate at ignition of the motor will be higher than the values based on average burn rate that are plotted in Figure 6. Summarizing, it is very difficult and requires careful set-up of the propellant characterization test to accurately measure the instantaneously high initial burn rate when threshold values are exceeded and erosive burning is present.

Note that the characteristic shape of the increase in burn rate with mass flux once the threshold mass flux is exceeded as was seen in Figure 5 is somewhat camouflaged in Figure 6, because as the chamber pressure increases the threshold mass flux for mass flux-based erosive burning also increases, see Figure 5 and Table 3. But eventually for the data plotted in Figure 6 the increase in the core mass flux overtakes the increase in the threshold mass flux with chamber pressure to create the characteristic increased burn rate with mass flux shape which can be clearly seen in Figure 6. Note that the threshold mass flux at a given chamber pressure is finally exceeded at a mass flux of  $1.8 \text{ lb/sec-in}^2$  at a  $p_c = 1297$  psia, values nicely bracketed by the chamber pressure/threshold mass flux design criteria for the onset of mass flux-based erosive burning presented

	$\rho_c = 409$ psia Non-Erosive	$\rho_c = 933.4$ psia Non-Erosive	Core Mass Flux 1.05 lb/sec-in <sup>2</sup>	Core Mass Flux 1.8 lb/sec-in <sup>2</sup>	Core Mass Flux 2.3 lb/sec-in <sup>2</sup>	Core Mass Flux 3.4 lb/sec-in <sup>2</sup>
Core Mach Number ( $M_a$ )	0.22	0.22	0.17	0.22	0.33	0.45

**Table 4. Core Mach Numbers for Test Motors Fired for CSXT D8 Propellant Characterization Tests.**

previously ( $\rho_c = 800$  psia, threshold mass flux 1.75 lb/sec-in<sup>2</sup>;  $\rho_c = 1400$  psia, threshold mass flux 2.0 lb/sec-in<sup>2</sup>) based on data from Figure 5 and Table 3.

The core Mach number (core Mach number at the aft end of the core) at ignition for each of the test motors fired for the CSXT D8 propellant characterization tests are presented in Table 4. The two non-erosive test motors and the four mass flux-based erosive burning characterization test motors correspond with the burn rate with chamber pressure and mass flux data plotted in Figure 6.

Note that the core Mach numbers for the non-erosive test motors were clearly non-erosive ( $M_a < 0.50$ ). The core Mach numbers for the erosive burning test motors were also non-erosive ( $M_a < 0.50$ ) in terms of velocity-based erosive burning. While the erosive burning test motors were non-erosive and then erosive in terms of core mass flux, they were non-erosive in terms of core Mach number, because the point of the tests was to quantify mass flux-based erosive burning with no velocity-based erosive burning present. It's also interesting to note that four out of the six core Mach numbers in Table 4 (core Mach numbers 0.17-0.22) cover the velocity region of about one-half the threshold velocity ( $0.5u_{tv}$ ) where the dip in the propellant burn rate with combustion gas velocity seen in Figure 3 would be predicted to occur. It's apparent for the CSXT D8 propellant data plotted in Figure 6 that for core Mach numbers equivalent to one-half the threshold velocity to core Mach numbers approaching the threshold core Mach number ( $(M_a)_{tv} = 0.50$ ) equivalent to the threshold velocity, no dip in the propellant burn rate is apparent in Figure 6. Variations in the propellant burn rate are clearly only a function of chamber pressure and mass flux.

important that the non-erosive core Mach number and core mass flux design criteria presented previously be followed to insure that the propellant characterization test motors are non-erosive. Previously most experimental/amateur rocketeers thought that after getting the core Mach number below the threshold value (the non-erosive core Mach number limit) for velocity-based erosive burning, that the lower the core Mach number, the better. The dip in propellant burning rate at low combustion gas velocities shown in Figure 3 opens up the possibility that when performing propellant characterization tests that experimental/amateur rocketeers will assume that they are measuring the non-erosive propellant burning rate, when they may in actuality be measuring a lower propellant burning rate from the dip in the propellant burning rate versus combustion gas velocity curve in Figure 3. Clearly all non-erosive propellant characterization tests should be performed with a core mass flux clearly below the threshold mass flux for the onset of mass flux-based erosive burning for the chamber pressure at which the test is being performed. Despite the fact that the present author, for the various propellant characterization tests he has participated in, has never seen the phenomenon of the dip in propellant burning rate shown in Figure 3, and that this dip in propellant burning rate at low velocities/low core Mach numbers is not present in the CSXT propellant characterization data presented in Figure 6, the present author recommends for experimental/amateur rocketeers that when performing propellant characterization tests for new propellants that two sets of tests with the test motors having core Mach numbers of 0.25 and 0.50 be performed to confirm that the dip in propellant burning rate at low velocities/low core Mach numbers is not present.

### **Core Mach Number and Core Mass Flux for Non-Erosive Propellant Characterization Tests**

When performing propellant characterization tests to determine the non-erosive internal ballistic characteristics of a propellant (chamber pressure versus  $K_n$ , burn rate versus chamber pressure), it's

## **Recommended Design Method — Non-Erosive Internal Ballistics Simulation Programs Combined with Erosive Burning Design Criteria**

### Non-Erosive Internal Ballistics Simulation Programs Combined with Erosive Burning Design Criteria

The detailed modeling of erosive burning in computer simulations of solid rocket motors is quite complex, and even with the creation of detailed erosive burning models extensive calibration of the models is required. Comparisons of predicted thrust-time curves with actual thrust-time curves over a series of erosive burning tests are required to fully calibrate the models. On the other hand there are many non-erosive internal ballistics solid rocket motor computer simulations available to the high power and experimental/amateur rocket communities. The first internal ballistics solid rocket motor simulation program released to the high power and experimental/amateur rocket communities was the ENGMOD program developed by the present author and Fred Brennon and released in 1988. Many internal ballistics solid rocket motor simulation programs are now available to high power and experimental/amateur rocketeers, and many experimental/amateur rocketeers use Microsoft™ Excel™ spreadsheets to perform these calculations.

In internal ballistics solid rocket motor simulation programs the motor grain geometry inputs are used to calculate the propellant burning surface area. The propellant burning surface area is then divided by the throat area to determine the motor  $K_n$ . Using stored or inputted propellant internal ballistic characteristics (chamber pressure versus  $K_n$ , burn rate versus chamber pressure), the chamber pressure is determined given the  $K_n$ . With the chamber pressure and atmospheric pressure and using a thrust coefficient model the thrust is determined. The chamber pressure is then used with the propellant internal ballistic characteristics to determine the propellant burning rate. With the propellant burning rate applied over a given time step the propellant burning surfaces are receded, the new propellant burning surface area is determined, and the computational process begins again until the propellant burning surfaces reach the case (or propellant liner) inner wall. Note that in these non-erosive internal ballistics motor simulation programs erosive burning is not included, all propellant burning surfaces have the same non-erosive propellant burning rate.

The design method recommended by the present author is to combine non-erosive internal ballistics

solid rocket motor simulation programs with erosive burning design criteria. This method takes advantage of the large body of non-erosive internal ballistics solid rocket motor simulation programs available to high power and experimental/amateur rocketeers, by taking the application of these programs to a new level through the application of erosive burning design criteria to the design of the motors run on the simulation programs.

Using the recommended combined core Mach number/core mass flux non-erosive design criteria which will be presented, the experimental/amateur rocketeer can design solid rocket motors which will have little or no erosive burning. These solid rocket motor designs can then be run on existing non-erosive internal ballistics simulation programs for accurate predictions of the motor thrust-time curve. Combined core Mach number/core mass flux design criteria will also be presented for the maximum amount of erosive burning recommended by the present author. Even for these maximum recommended erosivity motor designs, non-erosive internal ballistics solid rocket motor simulation programs can be used for the overall design of the motor and will produce reasonable predictions for the overall total impulse of the motor, although there will be substantial mispredictions in the initial thrust and the tail-off of the motor due to erosive burning. Even for maximum recommended erosivity motor designs, combining erosive burning design criteria with non-erosive internal ballistics solid rocket motor simulation programs can result in an effective solution to the erosive burning solid rocket motor design problem.

### Erosive Burning Design Criteria Based on Core Mach Number and Core Mass Flux at Aft End of Core at Motor Ignition

The highest combustion gas velocity and the highest mass flux in the core of a solid rocket motor will be reached at the aft (nozzle) end of the core at motor ignition. Thus the threshold values for velocity ( $u_{iv}$ ) and mass flux ( $G_{iv}$ ) for velocity-based erosive burning and mass flux-based erosive burning will be reached first at the aft end of the core. If the threshold values for velocity or core mass flux for erosive burning are exceeded prior to the aft end of the core, the highest velocity-based or mass flux-based erosive burning will occur at the aft end of the core. As noted in a previous section, core Mach number is a much more useful parameter than velocity, with the core Mach number also reaching its maximum value at the aft end of the core at motor ignition. Thus the present author proposes that the only core Mach number or core mass flux of interest for

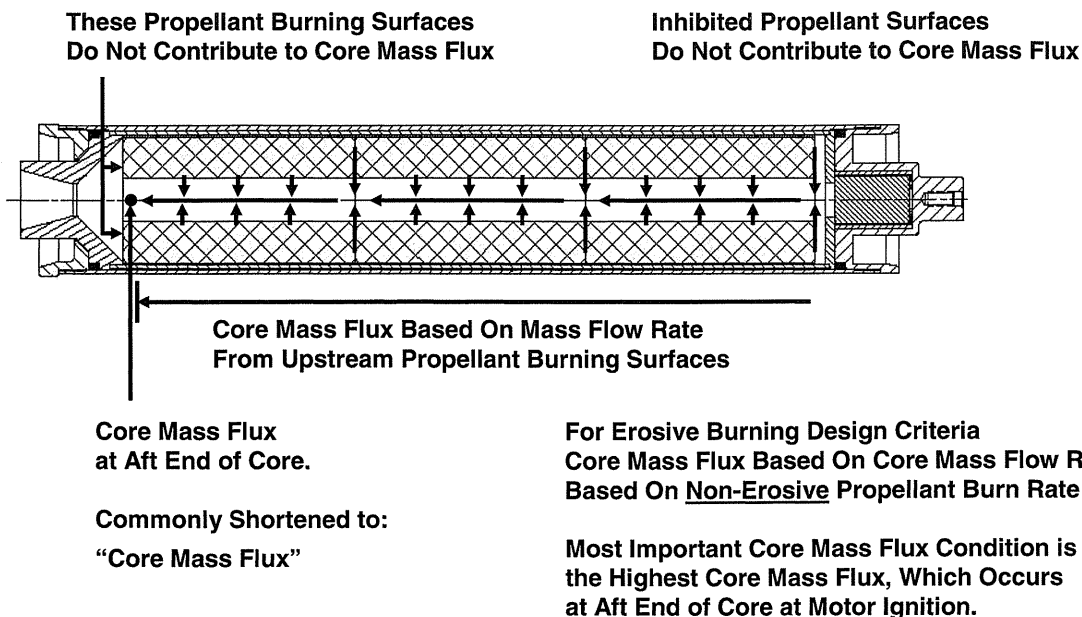


**Figure 7. Propellant Burning Surfaces Contributing to Core Mass Flux at Aft End of Core. Core Mass Flux Based on Non-Erosive Burn Rate.**

erosive burning design criteria are the core Mach number and core mass flux at the very end (the aft end) of the core at motor ignition.

The core Mach number at the aft end of the core is determined using Eq. (7). The core Mach number design criteria, based on the core Mach number at the aft end of the core, were presented previously.

#### Core Mass Flux at Aft End of Core Based on Non-Erosive Burn Rate

Figure 7 shows the mass flows from the various propellant burning surfaces which combine to form the total mass flow rate for the core mass flux at the aft end of the core. Any inhibited propellant surfaces do not contribute to the core mass flux. Note that the aft-facing propellant surfaces located aft (downstream) of the end of the core do not contribute to the mass flow rate in the core, and hence do not contribute to the core mass flux.

An important technique now introduced by the present author is to calculate the core mass flux at the aft end of the core (the "core mass flux" for the motor) for motor ignition only, and to base the core mass flux on the propellant flow rate based on the non-erosive burn rate. The highest core mass flux, and thus the highest mass flux-based erosive burning will be at motor ignition. Using the mass flow rate down the core based on the non-erosive burn rate greatly simplifies the calculation of the core mass flux, since including the effect that upstream erosive burning increases the mass flux for down-

stream propellant surfaces greatly complicates the calculation of the core mass flux. If the core mass flux limit for a given chamber pressure for non-erosive burning is not exceeded, then the fact that the core mass flux calculations were done assuming a non-erosive propellant burning rate will have no effect since there will be no erosive burning anyway. Using the recommended core mass flux design criteria and through experience the experimental/amateur rocketeer can calibrate what level of core mass flux based on non-erosive propellant burning rates produces acceptable levels of erosive burning.

From conservation of mass, the mass flow rate through the aft end of the core will be equal to the mass flow rate of the propellant being consumed from the propellant burning surfaces. Including only the propellant burning surfaces upstream of the aft end of the core, and as recommended by the present author using the non-erosive propellant burning rate ( $r_0$ ), the core mass flux equation, Eq. (3),

$$\text{Eq. (3):} \quad G = \dot{m}'_b / A_p$$

and the core mass flow rate now become;

$$\dot{m}'_b = A'_b r_0 \rho_p \quad (8)$$

$$G = A'_b r_0 \rho_p / A_p \quad (9)$$

Where:

$A'_b$  = propellant burning surface area upstream of aft end of core, m<sup>2</sup> (in<sup>2</sup>)

(Propellant burning surface areas downstream of aft end of core shown in Figure 7 are not included.)

$\rho_p$  = propellant density, kg/m<sup>3</sup> (lb/in<sup>3</sup>)

Since the propellant burning surface area downstream of the aft end of the core that is not included in  $A'_b$  (shown in Figure 7) is a small part of the total propellant burning surface area ( $A_b$ ), for quick approximate calculations the propellant mass flow rate based on the total propellant burning surface area  $A_b$  can be used in place of the propellant mass flow rate based on  $A'_b$  in Eqs. (8) and (9), which also allows the core mass flux calculations to be tied directly to the motor  $K_n$ .

With  $\dot{m}'_b \equiv \dot{m}_b$ , Eqs. (3), (8) and (9) now become;

$$G = \dot{m}_b / A_p \quad (10)$$

$$\dot{m}_b = A_b r_0 \rho_p \quad (11)$$

$$G = A_b r_0 \rho_p / A_p = K_n A_{th} r_0 \rho_p / A_p \quad (12)$$

Where:

$A_b$  = propellant burning surface area, m<sup>2</sup> (in<sup>2</sup>)  
(All propellant burning surfaces.)

$A_{th}$  = nozzle throat area (throat cross-sectional area), m<sup>2</sup> (in<sup>2</sup>)

$K_n$  = propellant burning surface area divided by throat area ( $A_b / A_{th}$ ), dimensionless

$\dot{m}_b$  = propellant mass flow rate, kg/sec (lb/sec)  
(Total propellant mass flow rate from all propellant burning surfaces.)

#### Combined Core Mach Number/Core Mass Flux Erosive Burning Design Criteria

The present author recommends that combined core Mach number/core mass flux erosive burning design criteria be used for high power and experimental/amateur solid rocket motors. As shown in Figure 8 the combined core Mach number/core mass flux erosive burning design criteria should be applied as follows:

- (1) The solid rocket motor should have a constant core diameter from the head end to the aft end of the core.
- (2) The initial sizing of the core port-to-throat area ratio ( $A_p / A_{th}$ ) is based on the non-erosive or maxi-

imum recommended erosivity core Mach numbers and port-to-throat area ratio values presented previously and repeated in Figure 8. The core Mach number limits are based on the core Mach number at the aft end of the core (Eq. (7)) at motor ignition.

(3) The initial (at motor ignition) core mass flux at the aft end of the core is determined based on the non-erosive propellant burning rate (Eqs. (8) and (9)), with the propellant burning surfaces aft of the end of the core not included (see Figure 7). For approximate calculations the entire propellant burning surface area can be used to calculate the core mass flux (Eqs. (10)-(12)).

(4) A design point core mass flux for the motor is established based on recommended non-erosive or maximum recommended erosivity core mass flux values presented previously and repeated in Figure 8.

(5) The initial core mass flux at the aft end of the core is checked against the desired design point core mass flux. If the design point core mass flux is exceeded, the motor core is opened up (the motor core diameter is increased) until the initial core mass flux is reduced to the design point core mass flux value.

The primary advantage of using combined core Mach number/core mass flux erosive burning design criteria for either non-erosive or maximum recommended erosivity motor designs is that irregardless of whether the motor propellant is susceptible to velocity-based or mass flux-based erosive burning, provisions for both have been included as both core Mach number limits and core mass flux limits have been considered in the sizing of the motor core.

#### **Constant Core Mass Flux Core Design**

An improved solid rocket motor core design proposed by the present author, that for a given level of erosivity maximizes the length and thus L/D of a motor, or maximizes the amount of propellant installed in a motor for a given length, is the constant core mass flux core design. Once a level of erosivity is established for the overall motor design, the constant core mass flux core design maximizes the amount of installed propellant to maximize the performance of the motor.

As shown in Figure 9, when using a constant core mass flux core design, once a design point core mass flux is achieved based on the level of erosivity the motor is being designed to, the core is then opened up (the core diameter is increased) to main-

# Combined Core Mach Number/Core Mass Flux Erosive Burning Design Criteria for Motors with Constant Diameter Cores

Step 1:

Initial Core Diameter Sized Based On  
Core Mach Number

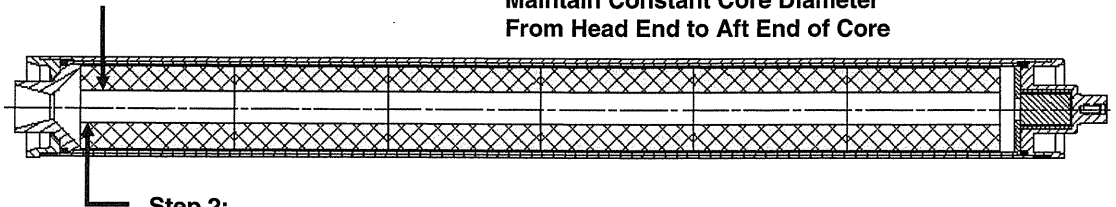
Non-Erosive;  $M_a = 0.50$   
 $\gamma = 1.2$ ;  $A_p/A_{th} = 1.36$

Max Erosive;  $M_a = 0.70$   
 $\gamma = 1.2$ ;  $A_p/A_{th} = 1.10$

Core Mach Number and Core Mass Flux  
Conditions are at Motor Ignition

Core Mass Flux Values Based on  
Non-Erosive Propellant Burn Rate

Maintain Constant Core Diameter  
From Head End to Aft End of Core



Step 2:

Check Core Mass Flux at Aft End of Core

If Core Mass Flux at Aft End of Core Higher Than Design Point Core Mass Flux,  
Increase Core Diameter to Reduce Core Mass Flux to Design Point Value.

Design Point Core Mass Flux (Recommended Values)

Non-Erosive; $p_c = 400-600$ psia	Core Mass Flux $\leq 1.0$ lb/sec-in <sup>2</sup>
$p_c = 800$ psia	Core Mass Flux $\leq 1.75$ lb/sec-in <sup>2</sup>
$p_c = 1400$ psia	Core Mass Flux $\leq 2.0$ lb/sec-in <sup>2</sup>
Max Erosive; $p_c = 400$ psia	Core Mass Flux = $2.0$ lb/sec-in <sup>2</sup>
$p_c = 600$ psia	Core Mass Flux = $2.5$ lb/sec-in <sup>2</sup>
$p_c \geq 800$ psia	Core Mass Flux = $3.0$ lb/sec-in <sup>2</sup>

**Figure 8. Combined Core Mach Number/Core Mass Flux Erosive Burning Design Criteria for Motors with Constant Diameter Cores.**

tain the same core mass flux down the rest of the core. As more propellant burning surface area is added down the core, the core has to be proportionately opened up to hold the core mass flux constant.

As shown in Figure 9 the constant core mass flux core design is implemented as follows:

(1) Initially a constant core diameter is used from the head end to the aft end of the core.

(2) The initial sizing of the core port-to-throat area ratio ( $A_p/A_{th}$ ) is based on the non-erosive or maximum recommended erosivity core Mach numbers and port-to-throat area ratio values presented previously and repeated in Figure 9.

(3) A design point core mass flux for the motor is established based on recommended non-erosive or maximum recommended erosivity core mass flux

values presented previously and repeated in Figure 9.

(4) Based on the non-erosive propellant burning rate, the point down the core where the design point core mass flux is achieved is identified. For each point down the core where the core mass flux is calculated, only the upstream propellant burning surfaces are included in the calculated core mass flux.

(5) Once the design point core mass flux is achieved, the core diameter is increased to increase the port area (the core cross-sectional area) to maintain a constant core mass flux at the design point core mass flux value.

(6) All core mass flux values, and the opening up of the core to maintain a constant core mass flux, are based on the ignition core mass flux and the initial core geometry at ignition.

# Constant Core Mass Flux Core Design

Core Mach Number and Core Mass Flux  
Design Point Conditions are at Motor Ignition

Core Mass Flux Values Based on  
Non-Erosive Propellant Burn Rate

Provides Maximum Motor Length,  
Minimum Motor Core Diameter,  
Maximum Propellant Loading for  
a Given Level (Design Point) of  
Erosive Burning

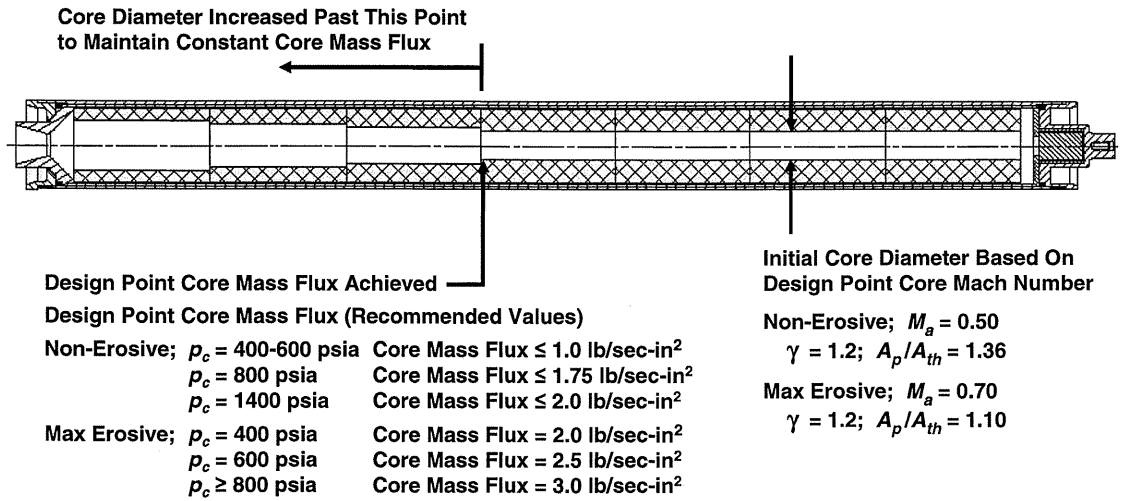


Figure 9. Constant Core Mass Flux Core Design.

(7) For the BATES grains used in the generic motor design presented in Figure 9, the last grain intersection upstream of the point where the design point core mass flux is achieved sets the point where all downstream grains will have their core diameters increased. Once the design point core mass flux is achieved, the core mass flux halfway down the length of each grain determines the required core diameter for each grain to maintain the constant core mass flux.

For the BATES grain generic motor design presented in Figure 9 the core mass flux versus motor length will "stair-step" in discrete steps as each subsequent grain core diameter increases based on the core mass flux halfway down the length of each grain. Note that the constant core mass flux core design can also be used for monolithic grains, where the port area can be gradually increased once the design point core mass flux is achieved, versus the step-wise increase in core diameter for the BATES grains in Figure 9.

## Effect of Core Complexity on Erosive Burning

An important note for the erosive burning material presented previously in this article is that the

velocity-based and mass flux-based erosive burning data presented in Figures 3 and 5, the core Mach number and core mass flux erosive burning design criteria developed from the data in Figures 3 and 5 and Tables 1 and 3, and the example mass flux-based erosive burning data for the CSXT propellant presented in Figure 6, are all for solid rocket motors with cylindrical cores (circular ports). Eq. (13) (from Ref. 1, original reference Ref. 7) provides a relative measure of configuration complexity for the core of a solid rocket motor.

$$X = Q^2 / (4\pi A_p) \quad (13)$$

Where:

$Q$  = burning perimeter of grain, m (in)

$X$  = configuration factor, dimensionless

For a grain with a circular port;

$$Q^2 = (2\pi r_c)^2$$

$$A_p = \pi r_c^2$$

$$X = Q^2 / (4\pi A_p) = (2\pi r_c)^2 / (4\pi^2 r_c^2) = 1.0$$

Where:

$r_c$  = core radius (circular port), m (in)

Thus a circular port has a configuration factor (X) of 1.0. For a non-circular port the configuration factor will be over 1.0. Generally grain geometries with more complex cores (a higher configuration factor) will be more susceptible to erosive burning, and will have more severe erosive burning if threshold Mach number or threshold core mass flux values are exceeded. Because of this core complexity effect, when designing motors with non-circular ports the erosive burning characterization tests for the motor propellant should be performed using test motors with the same core shape and the same configuration factor. If erosive burning characterization data for a propellant is based on test motors using cylindrical cores, and the propellant is then used in a motor using a grain design with a more complex core with a much higher configuration factor, significant errors in the predicted erosive burning may result.

## Summary

A solid rocket motor design method for high power and experimental/amateur rocket motors was presented where non-erosive internal ballistics solid rocket motor simulation programs are combined with erosive burning design criteria for the effective consideration of erosive burning design issues in the design of high power and experimental/amateur solid rocket motors. Design criteria for non-erosive and maximum recommended erosivity for velocity-based and mass flux-based erosive burning were presented. The use of core Mach number as a design criteria for velocity-based erosive burning, the use of the core Mach number and core mass flux at the aft end of the core as design criteria, and the basing of the core mass flux design criteria on the core mass flow rate based on the non-erosive propellant burning rate were presented. Combined core Mach number/core mass flux erosive burning design criteria were presented, which allow the effective design of non-erosive and erosive solid rocket motors whether the motor propellant is sensitive to velocity-based or mass flux-based erosive burning. Finally, a constant core mass flux core design was presented that once a given level of erosivity or non-erosivity has been set, maximizes the amount of propellant in a solid rocket motor and hence maximizes the motor performance. □

## Glossary

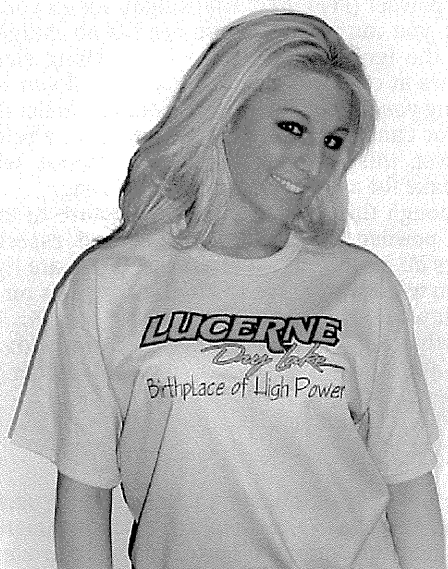
$a$	coefficient of pressure, also called burning rate constant
$a$	speed of sound, m/sec
$A_b$	propellant burning surface area, m <sup>2</sup> (in <sup>2</sup> )
$A'_b$	propellant burning surface area upstream of aft end of core, m <sup>2</sup> (in <sup>2</sup> )
$A_p$	port area (core cross-sectional area), m <sup>2</sup> (in <sup>2</sup> )
$A_{th}$	nozzle throat area (throat cross-sectional area), m <sup>2</sup> (in <sup>2</sup> )
$A_p/A_{th}$	port-to-throat area ratio, dimensionless
$G$	mass flux, kg/sec-m <sup>2</sup> (lb/sec-in <sup>2</sup> )
$G_{tv}$	threshold mass flux for the onset of mass flux-based erosive burning, kg/sec-m <sup>2</sup> (lb/sec-in <sup>2</sup> )
$K_n$	propellant burning surface area divided by throat area ( $A_b/A_{th}$ ), dimensionless
L/D	Length-to-Diameter ratio, dimensionless
$\bar{M}$	molecular mass, kg/kg-mol

$M_a$	core Mach number at aft end of core, dimensionless
$(M_a)_g$	Mach number for flow in motor core based on combustion gas velocity, dimensionless
$(M_a)_{tv}$	threshold Mach number for flow in motor core based on threshold velocity for onset of velocity-based erosive burning, dimensionless
$\dot{m}_b$	propellant mass flow rate, kg/sec (lb/sec)
$\dot{m}'_b$	propellant mass flow rate upstream of mass flux location, kg/sec (lb/sec)
$n$	burning rate pressure exponent
$p_c$	chamber pressure, Pa (lb/in <sup>2</sup> )
$Q$	burning perimeter of grain, m (in)
$R$	gas constant per unit weight, J/kg-°K
$R'$	universal gas constant, 8314.3 J/kg mol-°K
$r_b$	propellant burning rate, m/sec (in/sec)
$r_c$	core radius (circular port), m (in)
$r_e$	addition to propellant burning rate due to erosive burning, m/sec (in/sec)
$r_{th}$	nozzle throat radius, m (in)
$r_0$	non-erosive propellant burning rate, m/sec (in/sec)
$T$	absolute temperature, °K
$T_c$	adiabatic equilibrium flame temperature (combustion temperature), °K (°R)
$u_g$	combustion gas velocity, m/sec (ft/sec)
$u_{tv}$	threshold velocity for onset of velocity-based erosive burning, m/sec (ft/sec)
$X$	configuration factor, dimensionless
$\gamma$	ratio of specific heats, dimensionless
$\rho_p$	propellant density, kg/m <sup>3</sup> (lb/in <sup>3</sup> )

### References

1. *Solid Rocket Motor Performance Analysis and Prediction*, NASA Space Vehicle Design Criteria (Chemical Propulsion), NASA SP-8039, May 1971.
2. Zucrow, M. J., Osborn, J. R., and Murphy, J. M., *An Experimental Investigation of the Erosive Burning Characteristics of a Non-Homogeneous Solid Propellant*, AIAA Preprint 64-107, AIAA Solid Propellant Rocket Conference (Palo Alto, CA), January 29-31, 1964.
3. Sutton, George P., and Biblarz, Oscar, *Rocket Propulsion Elements*, 7th Edition, John Wiley and Sons, Inc., 2001.
4. "Solid Propellant Selection and Characterization," excerpts from NASA SP-8064 with additional material, forward by Rogers, Charles E., *High Power Rocketry Magazine*, Vol. 15, No. 6, February (A) 2001, pages 42-64, and Vol. 15, No. 7, February (B) 2001, pages 45-72.

5. Humble, Ronald W., Henry, Gary N., and Larson, Wiley J., *Space Propulsion Analysis and Design*, The McGraw-Hill Companies, Inc., 1995.
6. Kreidler, J. W., *Erosive Burning: New Experimental Techniques and Methods of Analysis*, AIAA Preprint 64-155, AIAA Solid Propellant Rocket Conference (Palo Alto, CA), January 29-31, 1964.
7. Fenech, E. J., and Billheimer, J. S., *Use of Internal Grain Configuration to Predict Erosive Burning Constant*, Paper 61-8, Western States Section, The Combustion Institute (Pacific Palisades, CA), April 1961.



**ROCKETEES**  
HIGH POWER SPORTSWEAR  
VISIT OUR WEBSITE AT  
[www.rocketees.com](http://www.rocketees.com)

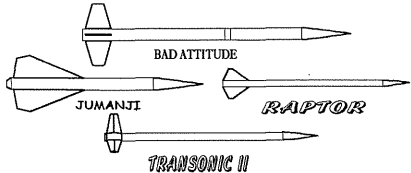
**FIBERGLASS ROCKET KITS  
BODY TUBES & FIN MATERIAL**

Why build a toy rocket out of cardboard when you can build a "Real Rocket" out of Fiberglass? Send \$2.50 for our catalog on fiberglass kits and accessories. Powdered Aluminum also available, As low as \$ 4.00/pound.

**G-12 Filament Wound Glass-Epoxy Body Tubes.**  
We carry popular sizes 29mm to 6".

**FR-4 Glass-Epoxy Sheets**  
FR-4 is the heat resistant version of G-10 and is better suited for fin material because of exhaust gases. These sheets are extremely strong with a tensile strength over 48,000 psi!

**Fiberglass Centering Rings**  
Aerospace grade Epoxy



**HAWK MOUNTAIN ENTERPRISES**  
Rd 1 Box 231 New Ringgold, PA 17960  
(570) 943-7644  
<http://www.hawkmountain.ws>

**TOP FLIGHT  
RECOVERY, LLC** ★

Since 1991  
[www.topflightrecoveryllc.com](http://www.topflightrecoveryllc.com)  
[tfr@execpc.com](mailto:tfr@execpc.com)

**PARACHUTES**  
**Crossfire- Heavy duty multi colored 6 panel chutes, flat braid nylon shroud lines.**

**Firewall - Nomex™ parachute & shock cord protectors.**

**Standard Chutes -Parachutes, X-type parachutes, streamers.**

**Fabric - Regular 1.7 oz. & 1.1oz. thin mill Ripstop nylon fabric in high visibility colors.**

**Swivels & Quick Links and other recovery supplies. Many sizes for model & high power rocketry.**

For catalog with complete product description & descent rate charts, send \$2.00 to:  
**TOP FLIGHT RECOVERY, LLC**  
S12621 Donald Road  
Spring Green, WI 53588  
(608) 588-7204



H  
I  
G  
H  
P  
O  
W  
E  
R  
R  
O  
C  
K  
E  
T  
R  
Y

# HIGH POWER ROCKETRY



\$5.95 CANADA \$8.50  
UK £4.25



FEATURES

**EROSIVE BURNING OF SOLID ROCKET MOTORS** | **PROJECT STUBBY** | **MONO-COPTER**